

Received October 20, 2019, accepted October 31, 2019, date of publication November 11, 2019, date of current version November 22, 2019.

Digital Object Identifier 10.1109/ACCESS.2019.2952879

# Research on Multi-Loop Nonlinear Control Structure and Optimization Method of PMLSM

RONGKUN WANG<sup>ID</sup>, FEI MAN<sup>ID</sup>, DONG YAN<sup>ID</sup>, BINGTAO HU<sup>ID</sup>,  
SIGUN SUN<sup>ID</sup>, QIYONG CHEN<sup>ID</sup>, AND JIE WANG<sup>ID</sup>

School of Information Science and Engineering, Huaqiao University, Xiamen 361000, China

Corresponding author: Rongkun Wang (wangrongkun@hqu.edu.cn)

This work was supported in part by the National Natural Science Foundation of China under Grant 51707068, in part by the Natural Science Foundation of Fujian Province under Grant 2017J01097, and in part by the Subsidized Project for Cultivating Postgraduates' Innovative Ability in Scientific Research of Huaqiao University under Grant 18014082013.

**ABSTRACT** Recently, the permanent magnet linear synchronous motor (PMLSM) servo control technology has become a research hotspot. However, the control performance under the traditional PID control is not ideal, which usually has the problems of slow response speed, large overshoot and poor anti-interference performance. In addition, adding nonlinear links with certain characteristics purposefully can greatly improve the performance of the system and achieve the expected effect that the traditional linear controllers cannot achieve. Based on this, this paper introduces the nonlinear PID control strategy into the field of servo control, and proposes a nonlinear control strategy of the three-loop of the servo system to improve the above problems. Firstly, the proposed structure is explained and the rule of nonlinear parameters selection is discussed. Secondly, the conditions for the structural stability of the proposed nonlinear control strategy are analyzed. Finally, experiments on the servo system platform are carried out and the results verify the fast dynamic response, precise positioning and good anti-disturbance performance.

**INDEX TERMS** Permanent magnet linear synchronous motor, nonlinear, tracking differentiator, multi-loop, servo.

## I. INTRODUCTION

Permanent Magnet Linear Synchronous Motor (PMLSM) has the advantage of high thrust, highly accurate positioning and fast speed, and it is gradually replacing the rotating electric machine to have a more widespread commercial value and further development [1]. Meanwhile, it also has higher requirements for the control technology of servo drive, and the traditional PID control cannot fully meet the complex needs of industry. However, PMLSM has strong nonlinear characteristics because its inductance, load and the changes of parameters. Therefore, the nonlinear control of PMLSM servo system has become a research hotspot. The nonlinear PID controller not only maintains the simple structure of the traditional PID controller, but also has the characteristic of strong robustness, so as to achieve the expected effect that the traditional linear controller cannot achieve. Therefore, it is widely used in the motor control area.

The associate editor coordinating the review of this manuscript and approving it for publication was Ning Sun<sup>ID</sup>.

Due to the characters of simple structure and easy implementation, the traditional PID is widely used in control systems, especially for the accurate mathematical models. Reference [2] adopts the linear PID in PMLSM, realizing good control of servo systems. However, the effect is not ideal, and traditional PID is especially suitable for the deterministic system instead of the controlled systems with nonlinear, coupling and load disturbance characteristics. In [3], the velocity loop of PMLSM servo system develops PID structure based on the Elman neural network, which achieves a relatively good tracking ability. However, the algorithm is easy to fall into the pole value. In [4], in order to solve the contradiction between the anti-jamming performance and speed, a composite fuzzy immune PID method is proposed, which is used for the velocity loop to obtain a dynamic response and anti-interference, but it has a poor control performance on the overshoot. Reference [5] optimizes the PID control effect by adding the BP neural network, but there are still large disturbances and long speed response time.

Reference [6] summarizes the defects of the classical PID controller and the corresponding improvement measures from four aspects, providing more theoretical possibilities for the control structure. However, there are little practical applications. In [7], the use of nonlinear PID controller is introduced to improve the performance of PAM manipulator, which can achieve good state. But due to the existence of differential signal, the noise has amplified effect, the ability to resist noise interference is poor. Reference [8] discusses a nonlinear tracking differentiator(TD) to deal with the non-linearity caused by noise, but there are weaknesses with complicated structure and many parameters, the structure is not easy to realize. In [9], a tracking differentiator based on classical PID control is introduced in PMLSM to solve the contradiction between the speed response and overshoot. The PMLSM can quickly track the speed command without overshoot. However, differential extraction still has poor effects in noisy situations. Reference [10] proposes a nonlinear PID controller, which meets the control requirements for noise, but it does not explain the tuning rules of parameters, and parameters selection is time-consuming. Reference [11] uses error function that depends on the system input and system output to design a nonlinear PID controller. In this way, the nonlinear PID controller can change parameters value according to the output response, but it fails to discuss the nonlinear PID stability analysis. Reference [12] designs the current control in the current inner loop of the PMLSM servo system and verifies that the proposed method has a good dynamic response, but there is still a similar weakness on the stability analysis.

In the above research, considerations are made on the individual aspects of system performance and the controller design is improved. For high-precision servo systems, it is difficult to balance both the response speed and the overshoot suppression. And the analysis of the anti-disturbance performance of the servo system is relatively weak, lacking a comprehensive control strategy to improve the three aspects at the same time. In addition, for the research of nonlinear strategy applied to the field of servo control, there are relatively few studies on the parameter selection and stability analysis. Considering the above problems, this paper proposes a nonlinear control strategy of cascaded servo three-loop structure. Firstly, a nonlinear function is used to optimize it. Secondly, the parameter selection rules and stability performance of the controller are explained. In addition, the performance of the tracking differentiator is described comprehensively. Finally, the nonlinear PID control is cascaded to meet the requirements of the different loop. And the speed feedback is added to further accelerate the response.

The rest of paper is organized as follows: Section II introduced the mathematical model of PMLSM and the PID control. Section III proposes nonlinear PID control strategy, including the structure, the parameter selection rules and the stability analysis. Section IV designs nonlinear PID and applies to current loop, speed loop and position loop respectively, and then the

simulation results are discussed. The experimental results are in section V.

## II. CONVENTIONAL PMLSM CONTROL STRATEGY

### A. MATHEMATICAL MODEL OF PMLSM

Since the PMLSM is developed by the rotary motor along its radial direction, the structural similarity makes the linear motor equally suitable for similar analysis. To simplify the analysis, the effects of magnetic circuit saturation, iron loss and other factors are ignored. Besides, the air gap of the PMLSM is relatively large,  $L_d=L_q=L$  is adopted. Therefore, the mathematical model of the non-salient pole based PMLSM in the vector control mode is shown in Fig. 1.

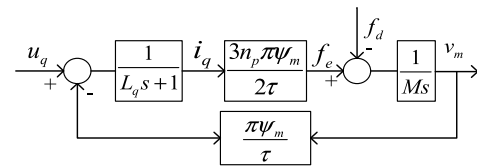


FIGURE 1. The model of PMLSM.

Where  $U_d$ ,  $i_q$ ,  $L_q$  are the voltage, current, and inductance of the q stator winding, respectively.  $\psi_m$ ,  $\omega_e$  are the flux of the permanent magnet and the synchronous rotational electrical angular velocity.  $F_e$  is the electromagnetic thrust.  $n_p$ ,  $\tau_p$  are the linear motor pole number and pole distance.  $M$  is the quality of load and mover.  $F_d$  is the load force.  $v_m$  is the speed.

In addition, from Fig. 1, it can be seen that there are accumulative terms in the stator voltage equation, so the nonlinear characteristics of the system can also be reflected.

### B. PMLSM THREE-LOOP CONTROL STRATEGY

In this paper, for the model of the surface-mount hidden PMLSM, the vector control mode of  $id=0$  is adopted to implement decoupling control, which can generate electromagnetic thrust with the minimum stator current and effectively reduce the loss [13]. A conventional three-loop control structure (current-speed-position [14]) is used, which is shown in Fig. 2.

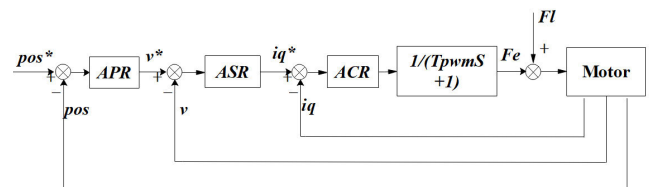


FIGURE 2. The structure of the conventional three-loop control.

The current loop, the innermost part of servo system, is aimed to control the stator current to track the reference value quickly and accurately [15]. The current loop is designed as an I-type system [16]. In order to obtain better dynamic performance, PI control is introduced into this loop. In order to guarantee the best value chosen, the principle of

Best Tuning Method of Siemens ( $\xi = 0.707$ ,  $KT = 0.5$ ) is used to adjust the current loop parameters, where  $\xi = 0.707$  is the damping ratio,  $K$  is the gain of open-loop and  $T$  is the system time constant [17].

The speed loop, which is aimed to suppress speed fluctuations to achieve good dynamic response and wide speed range [18], is designed as a Type II system. PI control is also introduced into speed loop. And the optimal parameters are selected according the principle of the minimum peak amplitude criterion of closed-loop amplitude-frequency characteristics in Oscillating Index Method.

The position loop, the outermost part of the system, is designed as a Type II system to track position rapidly. Besides, in order to avoid overshoot, only P control is introduced into position loop and the best value is selected by the principle of  $\xi = 1$ ,  $KT = 0.25$ . After the above discussion, combined with a theoretical derivation, the optimal parameters of three-loop are sure to select and it is shown in table 1.

TABLE 1. TD simulation parameters of pid.

parameter	value
Proportionality coefficient of current loop ( $k_{cp}$ )	0.433
Integral coefficient of current loop ( $k_{ci}$ )	0.542
Proportionality coefficient of speed loop ( $k_{sp}$ )	0.433
Integral coefficient of speed loop ( $k_{si}$ )	0.542
Proportionality coefficient of position loop ( $k_{pp}$ )	0.75

C. PROBLEM ANALYSIS

For the above traditional PID control, the frequency characteristics are analyzed, and the open-loop amplitude-frequency characteristic curve and the closed-loop amplitude-frequency characteristic curve are plotted, which are shown in the Fig. 3.

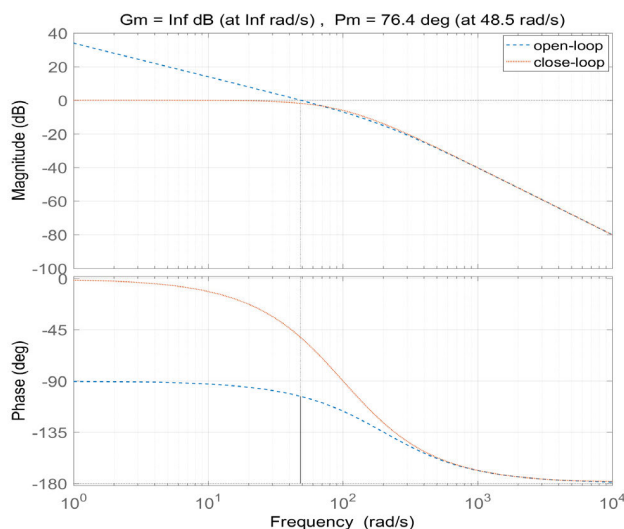


FIGURE 3. The analysis of the open-loop and closed-loop amplitude-frequency characteristics.

By the above observation, the system is stable under the “best” parameters (by the amplitude frequency

characteristics of the open loop), however, the response speed is relatively slow (by the amplitude frequency characteristics of closed loop), this is because the above principle of “best” followed is the biggest compromise parameter selection, is not really the best. However, for the servo system, the given value is random, and the output quantity is required to follow the quantitative change accurately. Therefore, on the basis of ensuring the stability of the system, its rapid response ability should be more prominent. In addition, generally, the nonlinear factors are harmful for the performance of the system, but the performance can be greatly improved by adding some nonlinear links with particular characteristics purposefully, to achieve the optimal effect that traditional linear controller does not achieve. Therefore, a nonlinear PID controller is used to improve the above performance. By selecting a kind of appropriate nonlinear function to adaptive change, the corresponding performance can be quickly responded with a smaller steady-state error. appropriate nonlinear control law, the system is also good for the anti-interference ability to the disturbance and the robustness is stronger.

III. NONLINEAR CONTROL

A. STRUCTURE OF NONLINEAR PID

The nonlinear PID controller improves the conventional PID by adopting a nonlinear control function [19], and it has faster response, smaller overshoot and smaller steady-state error. Nonlinear PID controllers can be roughly divided into two categories: the direct-action type and the gain-tuning type. The mathematical expression is characterized by [20]. As shown in Fig. 4, a direct-action nonlinear PID control structure is proposed by Han Jingqing [21].

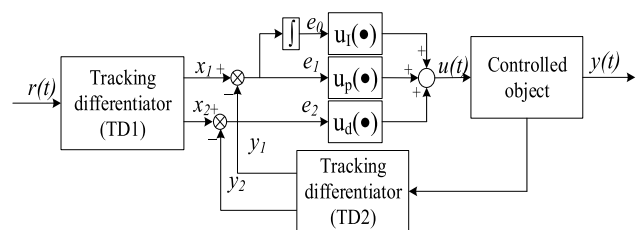


FIGURE 4. Block diagram of direct-action nonlinear PID control based on TD.

As shown in above, there are three parts consist of the nonlinear PID: tracking differentiator(TD), nonlinear gain function, and nonlinear control law.

1) TD

The function of TD is to follow the input signal as quickly as possible and to offer its differential signal, thus it is used to arrange the transient process. The aim is avoiding the shortcoming of the classical differentiator, that is, the noise amplification is so serious that the differential signal is submerged. And the advantage of the transient process is effectively solving the contradiction between rapidity and overshoot; the parameter selection range is expanded; and the robustness is stronger. TD provides an effective method

to extract differential signals in engineering [22]. And its discrete form is:

$$\begin{cases} x_1(k+1) = hx_2(k) \\ x_2(k+1) = x_2(k) + hfh \\ fh = fhan(x_1(k) - v(k), x_2(k), r, h_0) \end{cases} \quad (1)$$

where  $h$  is the tracking step of system,  $h_0$  is the filter factor,  $r$  is the speed factor, and  $u = fhan(x_1, x_2, r, h_0)$  is the time-optimal control function [18].

2) THE FUNCTION OF THE NONLINEAR GAIN

The function of  $fal(e, \alpha, \sigma)$  has a fitting adjustment characteristic of “large error, small gain; small error, large gain”, with a fast convergence capacity, and it is often used in nonlinear feedback structure. Therefore, it is much better than the linear function in the improving the systematic dynamic performance and the suppression of uncertain disturbance. And the structure is shown as follows:

$$fal(e, \alpha, \delta) = \begin{cases} |e|^\alpha \text{sign}(e), & |e| > \delta \\ \frac{e}{\delta^{1-\alpha}}, & |e| < \delta \end{cases} \quad (2)$$

In the formula,  $\alpha$  and  $\delta$  need to be adjusted.

3) THE LAW OF THE NONLINEAR CONTROL

The following feedback control rule is adopted to design the nonlinear combination:

$$\begin{cases} u = \beta_0 fal(e_0, \alpha_0, \delta) + \beta_1 fal(e_1, \alpha_1, \delta) + \beta_2 fal(e_2, \alpha_2, \delta) \\ \alpha_0 < 0 < \alpha_1 < 1 < \alpha_2 \quad \text{or} \quad 0 < \alpha_0 < \alpha_1 < 1 < \alpha_2 \end{cases} \quad (3)$$

Refer to (3), like the conventional PID, there are simply three parameters of  $\beta_0, \beta_1, \beta_2$  to be adjust.

4) SPEED FEEDFORWARD

In order to further improve the systematic response speed and suppress overshoot, and also avoid the problem of the systematic stability declining caused by a larger proportional coefficient, the feedforward correction of speed feedforward (kff) is added in the overall structure.

B. THE STABILITY OF NONLINEAR PID CONTROL

In this section, the stability of the nonlinear PID is analyzed. To simply process, the current loop, velocity loop and position loop in the PMLSM are designed as the low-order linear systems, respectively. Then, the overall systematic transfer function diagram is shown in Fig. 5.

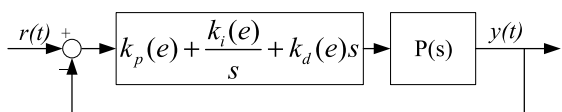


FIGURE 5. The transfer function block diagram of the low-order system nonlinear PID control system.

Where  $k_p(e), k_i(e), k_d(e)$  are nonlinear error functions and they are all positive numbers.

For first-order systems,  $P(s) = \frac{a}{bs+1}$ , and the closed-loop transfer function is:

$$G_1(s) = \frac{A[k_p(e)s + k_i(e) + k_d(e)s^2]}{[k_d(e) + B]s^2 + [Ak_p(e) + 1]s + Ak_i(e)} \quad (4)$$

According to the Hertz criterion, the parameters are stable in the range  $[0, +\infty)$ .

For second-order systems,  $P(s) = \frac{a}{s^2+bs+1}$ , and the closed-loop transfer function is:

$$G_2(s) = \frac{a[k_d(e)s^2 + k_p(e)s + k_i(e)]}{s^3 + [ak_d(e) + b]s^2 + [ak_p(e) + a]s + ak_i} \quad (5)$$

where  $a = \omega_n^2, b = 2\xi\omega_n, \omega_n$  is the natural oscillating angular frequency of second-order systems under the undamped condition and  $\xi$  is the damping ratio. According to the Routh table and the Routh criterion, the necessary and sufficient condition of the systematic stability is:

$$[b + ak_d(e)][k_p(e) + 1] > ak_i(e) \quad (6)$$

From (6), the system is globally stable when the P or PD control structure is adopted in nonlinear PID. And after adding the integral element, to ensure the stability of the system,  $k_i(e)$  should meet the following condition:

$$\max(k_i(e)) < [b + a \cdot \min(k_d(e))][\min(k_p(e) + 1)] \quad (7)$$

From (7), it can be seen that the addition of the D element can expand the range of systematic stability.

C. PARAMETER TUNING IN NONLINEAR CONTROL

1)Parameter Tuning of Nonlinear Feedback Control Rule The feedback control law, represented by (2), can be used for the nonlinear combination of a direct-action type. The effect of  $\alpha, \delta$  in  $fal(e, \alpha, \sigma)$  are shown in Fig. 6 and Fig. 7.

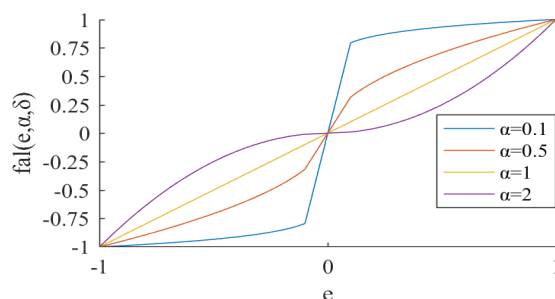


FIGURE 6. Output characteristics of  $fal(e, \alpha, \sigma)$  when  $\delta = 0.1$ .

Where  $\alpha$  is the error index that determines the nonlinearity of  $fal(e, \alpha, \delta)$ , that is, the tracking speed. And the larger the  $\alpha$  is, the stronger the nonlinearity and the faster the tracking speed will be.

$\delta$  is the demarcated point between the linear and the nonlinear region, which determines the size of the nonlinear interval. The smaller the  $\delta$  is, the larger the nonlinear interval will be, and the faster the systematic response speed will be. Meanwhile, the system will be more sensitive to changes of

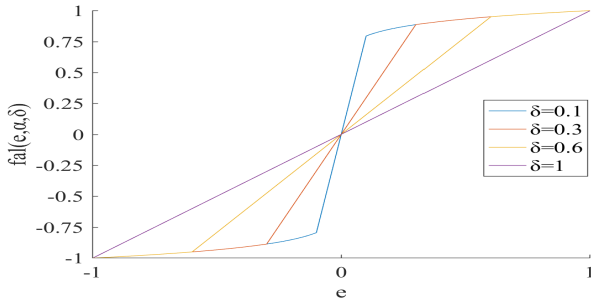


FIGURE 7. Output characteristics of  $fal(e, \alpha, \sigma)$  when  $\alpha = 0.1$ .

the control output. If a large interference exists, the system will easily oscillate.

2)Parameter Tuning of TD

For the tracking differentiator, taking  $h = T_s$ , then  $r$  and  $T_{ns}$  are adjusted to optimize the performance of TD [23]. Then, the output signals of TD are observed under the input step signal, the sinusoidal signal with different frequency and the sinusoidal signal with interference, respectively. The parameters selecting and simulation results of the step signal are shown in Table 2 and Fig. 8. The simulation results of the sinusoidal signal with different frequencies are shown in Fig. 9. And the simulation results of the sinusoidal signal with interference is shown in Fig. 10 and Fig. 11.

TABLE 2. TD simulation parameters.

Parameter	Input	$T_s$	$T_{ns}$	$r$
a	Step $V(t)=1$	0.000125	0.000125	$1e^5$
b	Step $V(t)=1$	0.000125	0.0002	$1e^5$
c	Step $V(t)=1$	0.000125	0.0002	$1e^7$
d	Step $V(t)=1$	0.000125	0.0002	$1e^8$

For the step input, the simulation results of Fig. 8 show that the larger the  $T_{ns}$  is, the smaller the oscillated amplitude of the TD output signal will be. According to the simulation, the effect is the best when  $T_{ns} = 1.6T_s$ . In addition, the larger  $r$  is, the faster the TD tracking speed will be, but there is a saturated value. If the value is exceeded, the tracking speed will vary little, and the excessive value will cause a jittered differential signal.

For the sinusoidal signal with different frequencies, results are shown in Fig. 9: as the sinusoidal frequency increasing, the phase shift and the amplitude of TD tracking signal will become larger and larger. This is caused by the hysteresis of the TD. For this problem, the feedforward is added for correction.

For the superimposed signal, the mixed signal (the Gaussian white noise with an amplitude of 0.1 and the sinusoidal signal with an amplitude of 1 and a frequency of 100Hz) is input into TD. Then the differential signal is extracted and compared with the differential signal which is extracted by the finite difference and the incomplete differential method, wherein the incomplete differential is one that is extracted

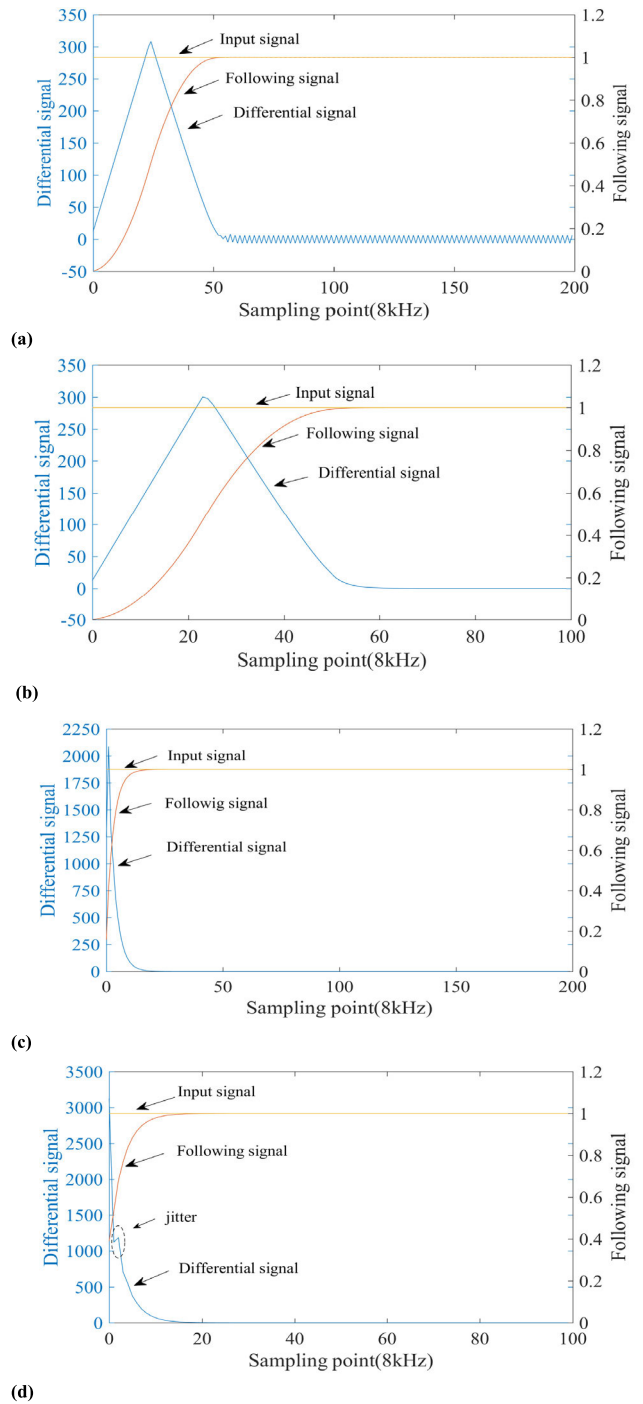
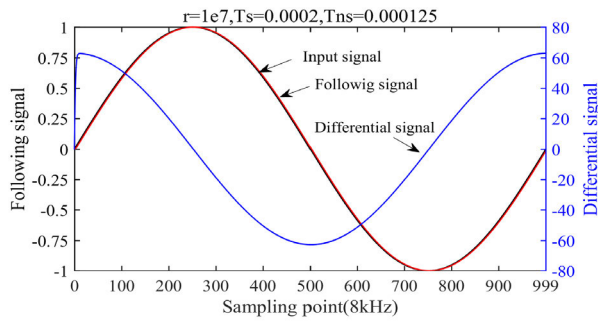
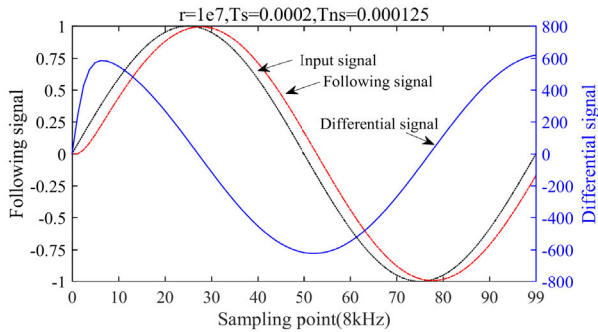


FIGURE 8. The response of TD under step-input.

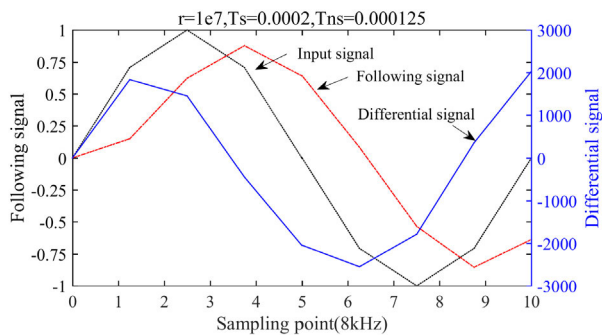
by finite difference and a low-pass filter with  $fc = 8kHz$ . Fig. 10 shows that the differential signal extracted by TD is better than that by simple finite difference. From Fig. 11, it can be seen that the differential signal extracted by incomplete differential is basically the same as the TD after the output is stable, but when the input is hopping (like an amplitude of 1 to 2 in the 50th sampling point set), the effect is much worse than the TD. This is because that the signal jumps, the differential signal extracted by incomplete differential is



(a)



(b)



(c)

FIGURE 9. The response of TD under sinusoidal input.

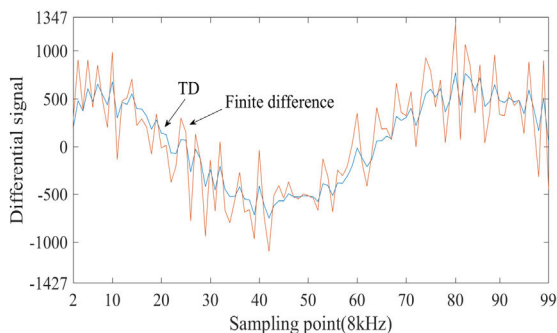


FIGURE 10. The results of finite difference and TD.

also hopping at the same time, while the differential signal generated by TD comes from the differential of the following signal, so there is a slow transiting process to the signal change, and it is not sensitive to the fluctuation of the input signal.

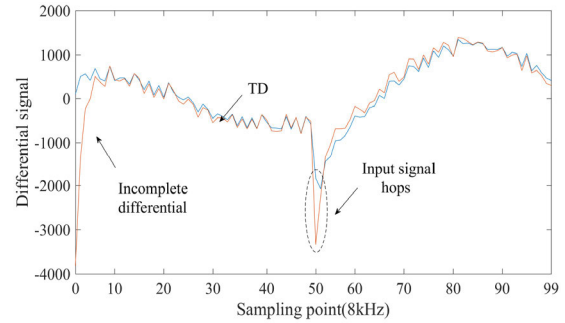


FIGURE 11. The results of incomplete differentiation and TD.

In summary, TDs can effectively extract differential signals, but there will produce large phase shifts and amplitude attenuations in high-frequency signals. Therefore, considering practical applications when using TDs is still recommended.

#### IV. THREE-LOOP CONTROL OF PMLSM BASED ON NONLINEAR PID

Under the two methods of nonlinear PID and traditional PID, the simulation and experimental verification of PMLSM are carried out. Finally, the control strategy based on nonlinear PID + feedforward control is proposed in this paper.

The parameters of AUM2-S1 (the linear motor platform for medical microscope) as the research object are shown in Table 3. To achieve a highly precise positioning control system, Mercury II 1600, with a resolution of 0.5um, an incremental encoder, is installed on the platform.

TABLE 3. AUM2-S1 liner motor parameters.

Category	Parameter
Rated current $I_R$ (A)	2
Peak current $I_{pk}$ (A)	8
Continuous power $P_R$ (W)	13
Peak power $P_{pk}$ (W)	208
Stator two-phase resistance $R_{AB}$ ( $\Omega$ )	3.25
Stator two-phase inductance $L_{AB}$ (mH)	0.75
Back electromotive force constant $K_e$ (V/m/s)	6.4

#### A. CURRENT LOOP

In order to achieve high steady-state control accuracy and fast dynamic response, the PI nonlinear control law from equation (8) is adopted in the current loop and the selected parameters are shown in Table 4. Fig. 12 shows the current response waveforms of traditional PID and nonlinear PID control.

$$u_i = \beta_{i0}fal(e_{i0}, \alpha_{i0}, \delta_i) + \beta_{i1}fal(e_{i1}, \alpha_{i1}, \delta_i) \quad (8)$$

As shown in Fig. 12, the current response curve of black line belongs to the nonlinear PID, and the green and blue

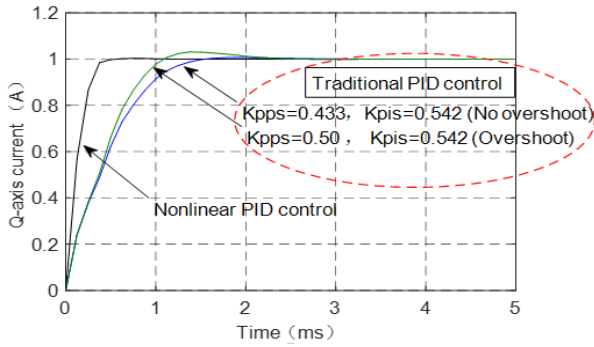


FIGURE 12. Comparison of current response.

TABLE 4. Current loop nonlinear control simulation parameters.

$\alpha_0$	$\alpha_1$	$\alpha_2$	$\delta$	$\beta_0$	$\beta_1$	$\beta_2$
0.1	0.75	1.5	0.2	0.16	0.4	0

curves belong to the traditional PID control, wherein the parameter of the green line is  $\xi = 0.707$  and there is overshoot; the parameter of the blue line is  $\xi = 1$  and there is no overshoot. It can be seen that there is a faster dynamic response without overshoot under the nonlinear PID. The rise-time of the Q-axis current is about 0.5ms, which has less time than the conventional PID. Considering the control effect, there is no need to add a TD and D element.

**B. SPEED LOOP**

The same structure of nonlinear PI control as the current loop is used to the speed loop. The nonlinear feedback rule adopted is characterized by:

$$u_v = \beta_{v0}fal(e_{v0}, \alpha_{v0}, \delta_v) + \beta_{v1}fal(e_{v1}, \alpha_{v1}, \delta_v) \quad (9)$$

In the formula,  $\beta_{v0} = 15, \beta_{v1} = 0.1$  is chosen and the nonlinear parameters are selected similarly as the speed loop. The step response waveforms of speed loop are shown in Fig. 13. From the figure, it can be concluded that the nonlinear PID has a faster response speed than PID and no overshoot.

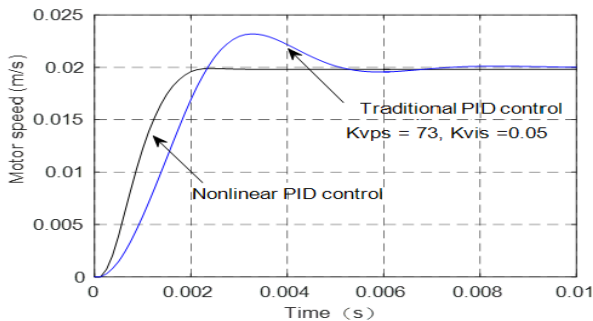


FIGURE 13. Comparison of speed step response.

**C. POSITION LOOP**

For the position loop, it differs from the speed loop by an integral operation. In general, the nonlinear control of P is simply used in position loop to avoid causing overshoots. However, due to the introduction of TD1 and TD2, PD control is adopted in the position loop to achieve the steady state without static difference. And the corresponding nonlinear feedback control rule is as follows:

$$u_p = \beta_{p0}fal(e_0, \alpha_{p0}, \delta_p) + \beta_{p2}fal(e_{v1}, \alpha_{p2}, \delta_p) \quad (10)$$

In addition, based on the above design, the speed feedforward is introduced into the system to further enhance the tracking performance and improve the phase-lagging problem generated by TD, which forms a composite control system together with the closed loop. Tuning parameters of the position loop are shown in Table 5. And the parameters of  $\alpha$  and  $\delta$  are set by the previous simulation.

TABLE 5. The nonlinear control simulation parameter of the position loop.

Symbol	Value	Symbol	Value
$\alpha_{p0}$	0.1	$h_1$	$2e^{-4}$
$\alpha_{p2}$	1.5	$h_2$	$2e^{-4}$
$\delta_p$	0.01	$r_1$	$1e^7$
$\beta_{p1}$	0.45	$r_2$	8.3
$\beta_{p2}$	0.4	$k_{ff}$	0.76

Finally, combined with the design of current loop and speed loop, the overall structure of PMLSM servo system is shown in the Fig. 14.

Given  $pos^* = 6000$ , the same actions of speed feedforward are worked on the nonlinear PID and the traditional PID, and the compared results are shown in Fig. 15.

Compared with the general PID, the nonlinear PID has a good effect on gentle transition and the suppressed overshoot of the given input (as shown in Fig. 15(a)); a faster tracking speed to meet a fast control (as shown in Fig. 15(b)); a smaller tracking error and steady-state error. In addition, it can be observed that the position error of the general PID is 4~5 times than that of the nonlinear PID in the three states (motor start-up state, first given arrival state and stable state), which shows that the nonlinear has a more excellent robust performance (as shown in Fig. 15(c)).

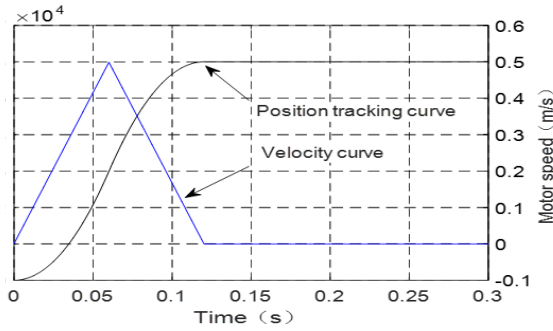
**V. EXPERIMENTAL VERIFICATION**

To realize the high-precision positioning control of PMLSM, the driver as the controller of TMS320F28335 is designed. The interrupt frequency of the control system is 8kHz. The maximum output power is 500W and the maximum current is 8A, which meets the application requirements of AUM2-S1. Fig. 16 shows the experimental system, where (a) is the connection of diagram blocks and (b) is the real system.

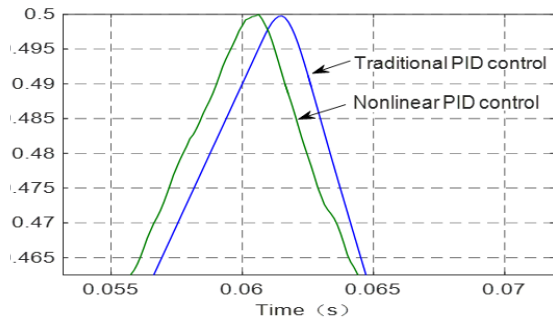
Considering the PMLSM control strategy of nonlinear PIDs with feedforward controls proposed in the previous



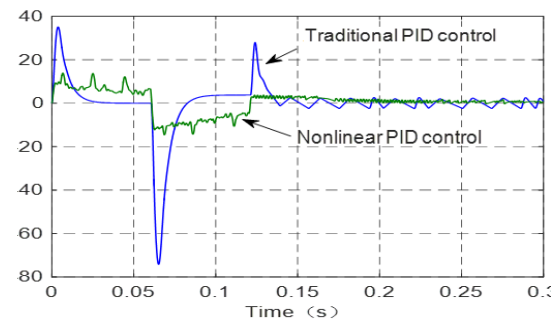




(a) Position and speed of motor



(b) Speed response

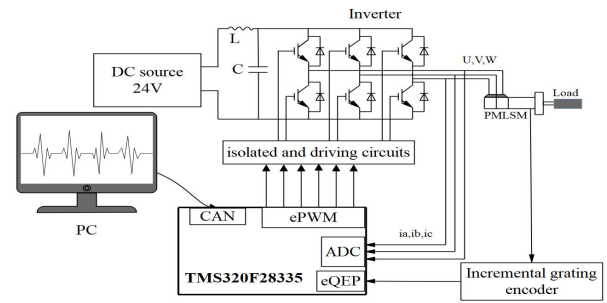


(c) Position tracking error

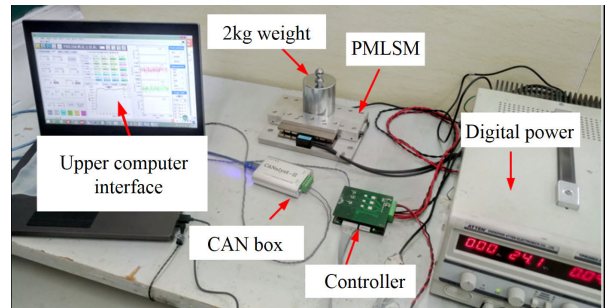
FIGURE 15. The position control effect comparison of nonlinear PID and conventional PID.

Then, under no-load conditions, the ramp signal with a ramp speed of 10 mm/s is input on the position loop. Limited by the grating position coordinates, positive and negative displacement limits are performed on the motor with the range value of  $[-70000, 70000]$ . Fig. 21 and Fig. 22 are the position feedback information and corresponding speed information, respectively. And Fig. 23 is the comparison of tracking error between PID control and the nonlinear PID control.

In Fig. 21, the motor tracks the given input signal accurately and randomly, and has a smooth transition of position. Besides, the information of speed in Fig. 22 also meets the performance requirement, in which some slight fluctuations are caused by the limited experimental conditions on certain friction. In Fig. 23, the position tracking error in conventional PID is smaller than the nonlinear PID, which shows that the nonlinear PID control has a smaller dynamic position tracking error. After loading 2kg on the PMLSM, it can be seen that



(a) diagram block



(b) real system

FIGURE 16. Experimental system.

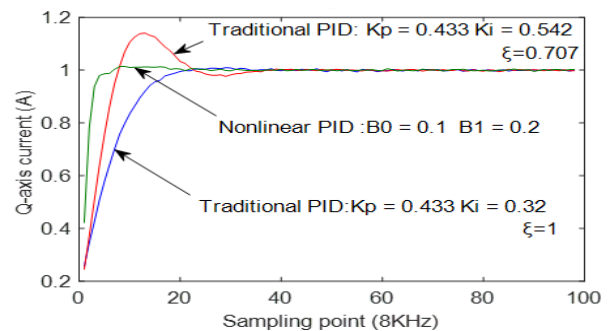


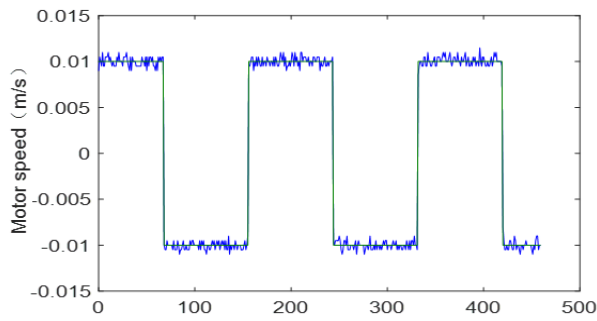
FIGURE 17. Step response when current is 1A.

the range under the conventional PID varies from  $\pm 0.2\text{mm}$  to  $\pm 0.4\text{mm}$ , while varies from  $\pm 0.1\text{mm}$  to  $\pm 0.2\text{mm}$  under the nonlinear PID. And the adjustment time of conventional PID is two times longer than the nonlinear PID.

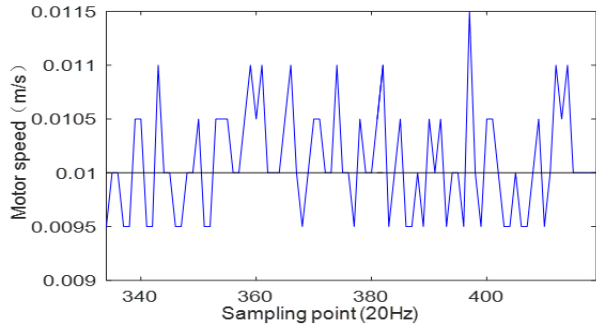
These experimental analyses show that, compared with PID, the motor under the nonlinear PID can track the random positioning better, and also has a faster response speed and a higher positioning accuracy. After adding the disturbance, under the same amplitude fluctuations of motor, the control of nonlinear PID can more quickly reset motor to the original balanced state and has a better anti-interference performance.

#### D. THE EXPERIMENT OF LOAD POSITIONING

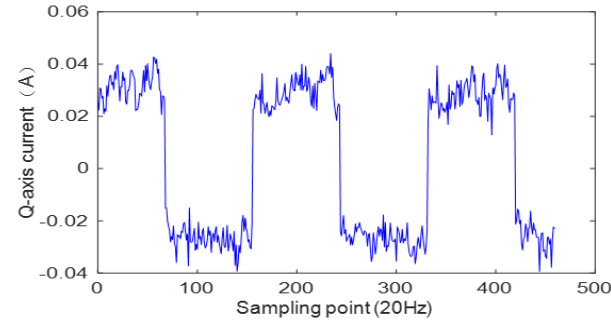
In practice, the study of PMLSM described in this paper is applied to an electric platform of a medical electron microscope, which is aimed to arrive at the pre-specified location quickly and accurately under load condition. Thus, a 2kg weight is put on the mover-component of the PMLSM to



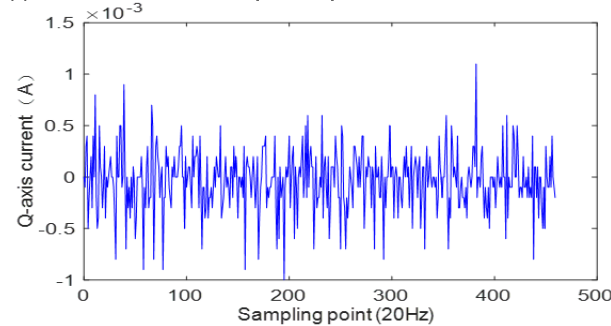
(a) Speed feedback and reference curve



(b) Partial magnification of the speed tracking steady-state curve



(c) Q-axis current under the speed loop



(d) D-axis current under the speed

FIGURE 18. Response waveforms under reciprocating motion.

simulate the actual working conditions and the positioning experiment is carried out by setting different positioning references. Under the load conditions, different positioning pulse lines are given to position experiments, and the tracking response curves are obtained through the host computer interface. Table 8 indicates the key value of the position-tracking curves that use 1, 10, 100 and 1000 pulses as the position

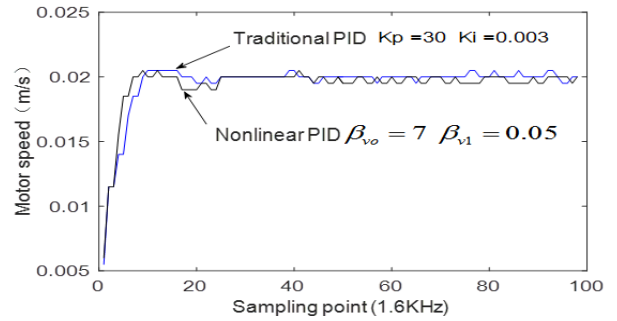


FIGURE 19. Speed step response.

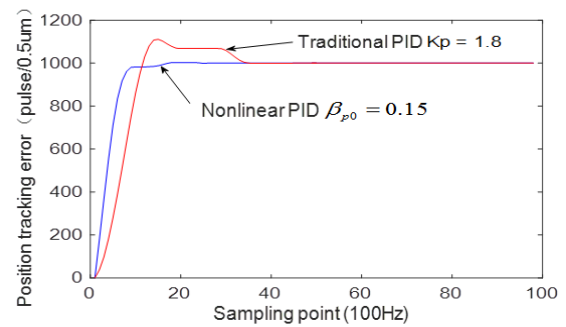


FIGURE 20. The step response of position loop under no-load condition.

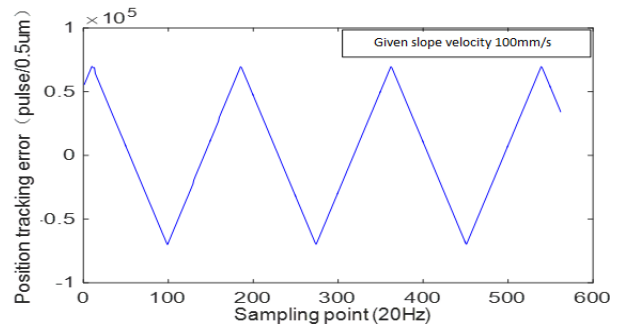


FIGURE 21. The position response of ramp given.

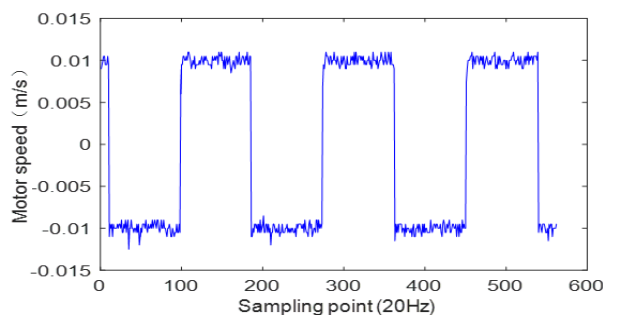


FIGURE 22. The corresponding information about speed.

reference. It can be seen that the PMLSM has a fast-dynamic response speed and accurate positioning accuracy under the current control strategy.

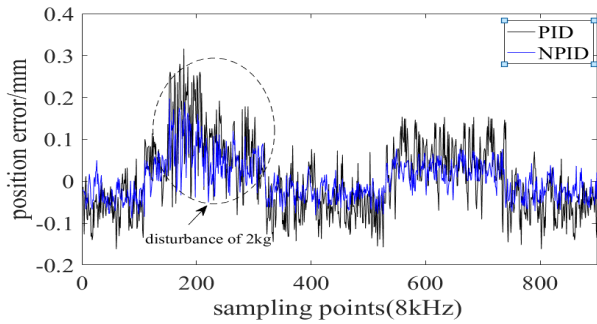


FIGURE 23. Position tracking error in reciprocating motion.

TABLE 8. The position-tracking curve parameters.

The number of minimum position pulse	Arrival time(s)	Position error
1	0.4	0
10	0.2	0
100	0.2	0
1000	0.25	0

## VI. CONCLUSION

The nonlinear control strategy combined with speed feedforward is adopted in this paper to control the research platform. Under the nonlinear PID control, the current loop has a faster response speed; the speed loop tracks the reference change quickly; the position loop can reach the specified position without overshoot quickly and accurately, and the good anti-disturbance performance is verified in the position loop. Experiments have shown that the proposed method has practical feasibility in the control of PMLSMs.

## ACKNOWLEDGMENT

The authors would like to thank their laboratory team members' assistance.

## REFERENCES

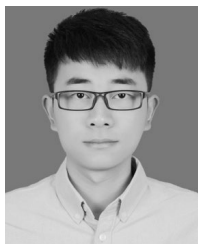
- [1] Y. Chou, L. Yu, and Y. R. Nan, "A survey for control strategy of permanent magnetism linear synchronous motors," *Small Special Electr. Mach.*, vol. 33, no. 10, pp. 39–43 Oct. 2005.
- [2] H. Wang, Y. Yu, and D. G. Yu, "The position servo system of PMSM," in *Proc. CSEE*, Jul. 2004, vol. 21, no. 7, pp. 151–155.
- [3] J.-M. Zuo, C. Pan, M.-L. Wang, and W. Su, "Elman dynamic neural network control for direct-drive feed system in advanced CNC machine tools," in *Proc. Int. Conf. Comput., Mechatronics, Control Electron. Eng.*, Changchun, China, Aug. 2015, pp. 307–310.
- [4] X. Zhishu, C. Tao, W. Guanghui, and X. Xing, "The CFI-PID controller design of PMLSM vector control system," in *Proc. 31st Chin. Control Conf.*, Hefei, China, Jul. 2012, pp. 4366–4371.
- [5] H. Wang, D. Zhang, and D. Wang, "Research of speed regulating system based on new intelligent PID control," *Micromotors*, vol. 47, no. 1, pp. 257–262, Jan. 2014.
- [6] J. Q. Han, *Active Disturbance Rejection Control Technique—The Technique for Estimating and Compensating the Uncertainties*. Beijing, China: National Defence Industry Press, 2007, pp. 243–254.
- [7] K. K. Ahn and T. D. C. Thanh, "Nonlinear PID control to improve the control performance of the pneumatic artificial muscle manipulator using neural network," *J. Mech. Sci. Technol.*, vol. 19, no. 1, pp. 106–115, Jan. 2005.
- [8] I. K. Ibraheem and W. R. Abduladheem, "On the improved nonlinear tracking differentiator based nonlinear PID controller design," *Int. J. Adv. Computer. Sci. Appl.*, vol. 7, no. 10, pp. 234–241, Oct. 2018.
- [9] G. Y. Yan, W. Ai, and B. Chen, "A nonlinear controller for PMLSM control system based on tracking differentiator," *Adv. Mater. Res.*, vols. 383–390, pp. 5796–5802, Jul. 2011.
- [10] K. K. Tan, T. H. Lee, and H. X. Zhou, "Micro-positioning of linear-piezoelectric motors based on a learning nonlinear PID controller," *IEEE/ASME Trans. Mechatronics*, vol. 6, no. 4, pp. 428–436, Dec. 2001.
- [11] M. Korkmaz, O. Aydoğdu, and H. Doğan, "Design and performance comparison of variable parameter nonlinear PID controller and genetic algorithm based PID controller," in *Proc. INISTA*, Trabzon, Turkey, Jul. 2012, pp. 1–5.
- [12] M. Wang, R. Yang, and C. Zhang, "Inner loop design for PMLSM drives with thrust ripple compensation and high-performance current control," *IEEE Trans. Ind. Electron.*, vol. 65, no. 12, pp. 9905–9915, Dec. 2018.
- [13] W.-J. Lin, "Comparison of two kinds of magnetic field oriented control strategies for permanent magnet synchronous motor," *Power Electron.*, vol. 41, no. 1, pp. 26–28, Jan. 2007.
- [14] L. Huang, X. Hao, X. Yang, T. Liu, R. Xie, and T. Liu, "Three-loop digital control strategy combining PI and quasi-PR controller for high tracking precision power supply used in ZnO characteristics testing," in *Proc. IFEEC*, Tainan, Taiwan, Nov. 2013, pp. 431–435.
- [15] J. Z. Liu, S. H. Hao, and T. Chen, "Research on the Current Loop of PMLSM," *Adv. Mater. Res.*, vols. 490–495, pp. 563–567, Mar. 2012.
- [16] Y. Okada, Y. Yamakawa, and T. Yamazaki, "Tuning method of PID controller for desired damping coefficient," in *Proc. SICE Annu. Conf.*, Takamatsu, Japan, Jan. 2008, pp. 795–799.
- [17] B. S. Chen, *Electric Traction Automatic Control System: Motion Control System*. Beijing, China: China Machine Press, 2003, pp. 68–70.
- [18] R. Chen, *Research on Permanent Magnet Synchronous Motor Servo System*. Jiangsu, China: Nanjing Aerospace Univ., 2004.
- [19] H. Huang, "Nonlinear PID controller and its applications in power plants," in *Proc. Int. Conf. Power Syst. Technol.*, Oct. 2002, pp. 1513–1517.
- [20] B. G. Hu, "A study on nonlinear PID controllers—Proportional component approach," *Acta Autom. Sinica*, vol. 32, no. 2, pp. 219–227 Mar. 2006.
- [21] J. Han, "Nonlinear PID controller," *Acta Automatica Sinica*, vol. 20, no. 4, pp. 487–490, Feb. 1994.
- [22] R. Cajo and W. Agila, "Evaluation of algorithms for linear and nonlinear PID control for twin rotor MIMO system," in *Proc. APCASE*, Quito, Ecuador, Jul. 2015, pp. 214–219.
- [23] F. Zhu and X. Chen, "Analysis and improvement of the nonlinear tracking differentiator," *Control Theory Appl.*, vol. 16, no. 6, pp. 898–902, Dec. 1999.



**RONGKUN WANG** was born in Fujian, China. He received the Ph.D. degree in electrical engineering from the Institute of Modern Physics, Chinese Academy of Sciences, in 2013. He is currently a master's Instructor with Huaqiao University. His current research interests include power electronics and power drives, devoting to digital UPS and its parallel technology, the control of the permanent magnet synchronous linear motors, harmonic detection method, and three-level active filter and other innovative research. He is a major participant in the study of major national science and technology projects and Chinese Academy of Sciences directional projects.



**FEI MAN** was born in Gansu, China. She is currently pursuing the master's degree with Huaqiao University. She was involved in electric drive and power conversion technology.



**DONG YAN** was born in Hunan, China. He is currently pursuing the master's degree with Huaqiao University. He was involved in electric drive and power conversion technology.



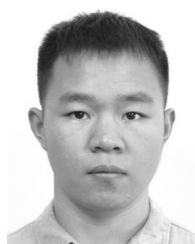
**QIYONG CHEN** was born in Fujian, China. He is currently pursuing the master's degree with Huaqiao University. He was involved in electric drive and power conversion technology.



**BINGTAO HU** was born in Anhui, China. He is currently pursuing the master's degree with Huaqiao University. He was involved in electric drive and power conversion technology.



**SIGUN SUN** was born in Fujian, China. He is currently pursuing the master's degree with Huaqiao University. He was involved in electric drive and power conversion technology.



**JIE WANG** was born in Fujian, China. He is currently pursuing the master's degree with Huaqiao University. He was involved in electric drive and power conversion technology.

...